Chinese Journal of Natural Medicines

Study on the dynamic variation of the secondary metabolites in *Viscum coloratum* using targeted metabolomics

Ruizhen ZHANG, Rong DUAN, Weiqing WANG, Zhiguo YU, Yun LI, Yunli ZHAO

Citation: Ruizhen ZHANG, Rong DUAN, Weiqing WANG, Zhiguo YU, Yun LI, Yunli ZHAO, Study on the dynamic variation of the secondary metabolites in *Viscum coloratum* using targeted metabolomics, Chinese Journal of Natural Medicines, 2023, 21(4), 308−320. doi: 10.1016/S1875−5364(23)60439−X.

View online: https://doi.org/10.1016/S1875−5364(23)60439−X

Available online at www.sciencedirect.com
ScienceDirect
Chinese Journal of Natural Medicines 2023, **21**(4): 308-320
doi: 10.1016/S1875-5364(23)60439-X
Chinese Journal of Natural Medicines

•Original article•

Study on the dynamic variation of the secondary metabolites in *Viscum coloratum* using targeted metabolomics

ZHANG Ruizhen[1], DUAN Rong[1], WANG Weiqing[1], YU Zhiguo[1], LI Yun[2*], ZHAO Yunli[1*]

[1] *Department of Pharmaceutical Analysis, School of Pharmacy, Shenyang Pharmaceutical University, Shenyang 110016, China;*
[2] *Department of Pharmacy, the Second Hospital of Dalian Medical University, Dalian 116023, China*

Available online 20 Apr., 2023

[ABSTRACT] *Viscum coloratum* (Kom.) Nakai is a well-known medicinal plant. However, the optimal harvest time for *V. coloratum* is unknown. Few studies were performed to analyze compound variation during storage and to improve post-harvest quality control. Our study aimed to comprehensively evaluate the quality of *V. coloratum* in different growth stages, and determine the dynamic variation of metabolites. Ultra-performance liquid chromatography tandem mass spectrometry was used to quantify 29 compounds in *V. coloratum* harvested in six growth periods, and the associated biosynthetic pathways were explored. The accumulation of different types of compounds were analyzed based on their synthesis pathways. Grey relational analysis was used to evaluate the quality of *V. coloratum* across different months. The compound variation during storage was analyzed by a high-temperature high-humidity accelerated test. The results showed that the quality of *V. coloratum* was the hightest in March, followed by November, and became the lowest in July. During storage, compounds in downstream steps of the biosynthesis pathway were first degraded to produce the upstream compounds and some low-molecular-weight organic acids, leading to an increase followed by a decrease in the content of some compounds, and resulted in a large gap during the degradation time course among different compounds. Due to the rapid rate and large degree of degradation, five compounds were tentatively designated as "early warning components" for quality control. This report provides reference for better understanding the biosynthesis and degradation of metabolites in *V. coloratum* and lays a theoretical foundation for rational application of *V. coloratum* and better quality control of *V. coloratum* during storage.

[KEY WORDS] *Viscum coloratum*; Harvesting period; Storage; Plant metabolomics; Quality control
[CLC Number] R917 **[Document code]** A **[Article ID]** 2095-6975(2023)04-0308-13

Introduction

Viscum coloratum (Komar.) Nakai, a semi-parasitic plant of *Viscum* L. and known as mistletoe, is a medicinal plant widely distributed in Asia. Its dry stems and leaves have long been used in traditional Chinese medicine (TCM). This plant was first recorded in *Shennong's Classic of Materia Medica* for the treatment of arthralgia, soreness of the waist and knees, and threatened abortion. In many pharmacological studies, *V. coloratum* exerted various pharmacological properties, such as anti-cardiovascular diseases [1-3], anti-tumor activity [4-7], immune regulation [8], anti-aging, anti-oxidation [9], inhibition of platelet aggregation [10], and anti-viral activities [11]. In recent decades, many metabolites have been extracted from *V. coloratum*, including flavonoids [12–15], triterpenes [16, 17], organic acids [17], lignans [18], and other compounds.

The active compounds of Chinese herbal medicines are usually secondary metabolites. Notably, secondary metabolism has a seasonal pattern, with specific metabolic activities that tend to be more active in a certain season. Therefore, the quality of medicinal materials can be guaranteed only when the medicinal plant grows to a certain period and are harvested within a certain period of time. For example, significant differences exist in the contents of steroid saponins in *P. polyphylla* var. *chinensis* across different growth years and harvest seasons. YIN *et al*. [19] found that the quality of *P. polyphylla* var. *chinensis* harvested in November was the best when it had been grown for at least eight years. LUO *et al*. [20] found that the content of cardiac glycosides in *Sophora flavescens* Alt. was the highest when harvested from October to December. Research by XUE *et al*. [21] showed that the total flavonoids and total phenolic acids in *Artemisia argyi* Levl. et Vant. exhibited the same change trend across six harvest periods. The type of medicinal plant, organ, growth characteristics, active ingredients, and dynamic changes in dry

[Received on] 12-Oct.-2022
[Research funding] This work was supported by Liaoning Revitalization Talents Program (No. XLYC1908031).
[*Corresponding author] E-mails: dlmuxh@126.com (LI Yun); Yunli76@163.com (ZHAO Yunli)
These authors have no conflict of interest to declare.

matter accumulation should be considered when determining the harvest time of a medicinal plant.

Due to the complex composition and structures of metabolites, medicinal materials are easily affected by the surrounding environment during storage, leading to the deterioration and waste of active components. Generally, the factors affecting the quality of Chinese herbal medicines can be divided into two categories: external factors and internal factors. External factors primarily refer to external conditions, such as temperature, humidity, light, air, and microorganisms. For example, physalis in *Physalis alkekengi* L. significantly decreased because of moisture, light, and high temperature [22], while the content of chlorogenic acid in Eucommia ulmoides Oliver was reduced to various degrees by temperature and light [23]. Internal factors refer to different types of compounds that are easily affected by various factors due to their different chemical structures, resulting in different forms of degradation or inactivation. For example, reduced anthraquinone compounds are easily oxidized, volatile components are easily volatilized under high temperature conditions, lignans are easily isomerized and inactivated under light, and glycosides are prone to hydrolysis [24]. The primary factor accounting for the deterioration of Chinese herbal medicines is the decreased contents of active ingredients. External factors also affect the structure of active ingredients, making it more vulnerable to degradation. Therefore, it is important to investigate the changes of active ingredients in Chinese herbal medicines during storage.

For *V. coloratum*, its harvest times has been recorded in TCM books written or compiled in the past dynasties. For instance, it was recorded as "harvest on March 3 and dried in the shade" in *Ming Yi Bie Lu* (*Symbol Miscellaneous Records of Famous Physicians*) and *Newly Revised Materia Medica*. *The Compendium of Materia Medica* stated that *V. coloratum* is "collected in July and August" and *Chinese Materia Medica* records it as "generally harvest in winter". The 2020 Chinese Pharmacopoeia stipulates "harvest from winter to next spring". Obviously, there are different opinions concerning the harvest time of *V. coloratum*, but the theoretical support for determination of the optimal harvest period of *V. coloratum* is insufficient. In terms of the storage conditions of *V. coloratum*, the Chinese Pharmacopoeia only stipulates that it should be "placed in a dry place to prevent insects". However, the metabolites can still be affected by other external factors. There are a few studies reporting the changes in metabolites in *V. coloratum* during storage, but theoretical evidence for post-harvest quality control is limited. Therefore, it is necessary to determine the pattern of metabolite changes during both the growth and storage of medicinal materials for better quality control.

At present, there are increasing researches concerning the metabolites in mistletoe. For example, Tatyana *et al*. [25] investigated non-polar and volatile compounds in *V. coloratum* and proved that the extract was cytotoxic to Ehrlich carcinoma cells. Dai *et al*. [26] isolated ten compounds from *Viscum album* and confirmed that three of them were cytotoxic. Our research group conducted a lot of studies on *V. coloratum*, including compound separation and biological activity studies [27, 28], establishment of a fingerprinting method to control the quality of *V. coloratum* [29], and exploring the relationship of compounds between the host and *V. coloratum* [30, 31]. We also looked in how the origin and host affected the chemical composition of *V. coloratum* [32]. But these studies simply focus on compound information at a certain time point, and may not reveal the changing law of metabolites in *V. coloratum* in a growth cycle. Therefore, based on existing research, it is difficult to determine which growth stage contribute to better quality of *V. coloratum*.

Medicinal plant-based metabolomics is a versatile tool which adopts a variety of analytical methods to comprehensively analyze the low-molecular-weight metabolites of medicinal plants and qualitatively and quantitatively determine the effects of genes or the environment on metabolites as a whole. The modern omic-technique attempts to systematically identify metabolic synthesis pathways, metabolite networks, and regulatory mechanisms, in order to provide a foundation for medicinal plant variety selection, new drug development, and quality and safety evaluation [33]. Grey relational analysis (GRA) is a method which uses the grade of relation to determine the similarity or difference degree between two sequences. The principle of evaluating sample quality by GRA is as follows: first, establishing an ideal reference sequence based on research data, and then evaluating the correlation between the test sample and the ideal sequence to evaluate sample quality. A close correlation between the sample and the ideal sequence indicates good sample quality [34].

The current study was designed to analyze the overall dynamic changes of compounds in mistletoe during the growth and storage periods, and to provide reference for the quality control of mistletoe and the study of biogenic synthesis pathways. In this study, *V. coloratum* was harvested every two months from March 2019 to January 2020, and 29 components in 36 batches of *V. coloratum* harvested across six harvest periods were quantified. The dynamic changes of the selected compounds were analyzed by comprehensively considering the structure of the compounds and the biosynthetic pathways involved, in order to provide theoretical support for determining the optimal harvest time for *V. coloratum*. GRA was used to evaluate the quality of *V. coloratum* in different months. In addition, a high-temperature and high-humidity accelerated test was designed, and the bioactive components of *V. coloratum* from different acceleration periods were quantified to explore their changes. These findings will provide reference for the quality control of *V. coloratum* after harvest.

Material and Methods

Chemicals and reagents

Methanol and formic acid (HPLC grade) were obtained from Tianjin Concord Technology Co., Ltd. (Tianjin, China).

Acetonitrile (HPLC grade) was purchased from Fisher Scientific (New Jersey, USA). Ultrapure water was purchased from Hangzhou Wahaha Group (Hangzhou, China).

Shikimic acid (Shik), eleutheroside E (Eleu), and salicylic acid (Sali) were purchased from Shanghai Acmec Biochemical Co., Ltd. (Shanghai, China). Succinic acid (Succ) and 4-hydroxycinnamic acid (Hydr) were purchased from WEIKEQI Biotechnology Co., Ltd. (Sichuan, China). Protocatechuic acid (Prot) was purchased from Must Biotechnology Co., Ltd. (Chengdu, China). Abscisic acid (ABA) was obtained from Mreda Technology Co., Ltd. (Beijing, China). Ferulic acid (Feru), chlorogenic acid (Chlo), paracetamol (APAP), coumarin (Coum) and sulfamethoxazole (SMZ) were purchased from the National Institute of Food and Drug Control (Beijing, China).

Phenylalanine (Phen), (1*E*,4*E*)-1,7-bis(4-hydroxyphenyl) hepta-1,4-dien-3-one (Dhdk), homoeriodictyol (Hedt-IV), 3,5-dihydroxy-1,7-bis(4-hydroxyphenyl)heptane (Dbhh), quercetin-3,3'-dimethyl ether (Quer), betulinic acid (Betu), oleanolic acid (Olea), homoeriodictyol-7-*O*-*β*-D-glucoside (Hedt-III), isorhamnetin-3-*O*-*β*-D-glucoside (Isor), rhamnazin-3-*O*-*β*-D-glucoside (Rham-I), syringenin 4-*O*-*β*-D-apiofuranosyl (1→2)-*β*-D-glucopyranosides (Syri-II), dihydrophaseic acid-4'-*O*-6"-(*β*-ribofuranosyl)-*β*-glucopyranoside (Dihy), (+)-lyoniresinol-3*α*-*O*-*β*-D-glucopyranoside (Lyon), homoeriodictyol-7-*O*-*β*-D-apiosiyl-(1→2)-*O*-*β*-D-glucoside (Hedt-II), rhamnazin-3-*O*-*β*-D-(6"-*β*-hydroxy-*β*-methyglutaryl)-glucoside (Rham-II), rhamnazin-3-*O*-*β*-D-(6"-*β*-hydroxy-*β*-methyglutaryl)-glucoside-4'-*O*-*β*-D-glucoside (Rham-III), syringin (Syri), pachypodol (Pach), and 5-hydroxy-3,7,3'-trimethoxylflavonoid-4'-*O*-*β*-D-glucoside (Httf) were obtained from our previous experiments, with a purity of more than 98% (HPLC grade).

Syri, Pach, Httf, Coum, and Eleu were detected in the positive ion mode, while the other compounds were detected in the negative ion mode. In addition, homoeriodictyol-7-*O*-*β*-D-apiosiyl-(1→5)-*β*-D-apiosyl-(1→2)-*β*-D-glucoside (Hedt-I) is another isolated flavonoid. Due to the lack of reference standards, Hedt-I was semi-quantitatively analyzed according to its theoretical ion fragments. Among these metabolites, Hedt-IV, Hedt-III, Hedt-II, Rham-I, Httf, Rham-II, Isor, Pach, Quer, Olea, Syri, Prot, Dhdk, Hedt-I, Rham-III, ABA, Dbhh, Shik, Sali, Phen, Chlo, Betu, Coum, Syri-II, Lyon, and Dihy were previously isolated or identified from mistletoe by our research group [27, 28, 31, 35]. Eleu, Hydr, Succ, and Feru were isolated from mistletoe by other researchers [12, 17, 18]. The structures of all analytes are shown in Fig. 1.

Preparation of standard solutions

First, the stock solution of each compound at 0.50 mg·mL^{-1} was obtained by dissolving the corresponding standard substance in 50% methanol. A positive mixed standard solution and a negative mixed standard solution were prepared by diluting an appropriate amount of stock solution of the corresponding compound in 50% methanol. The concentration of each compound in the negative mixed standard solution was listed as follows: Succ 20.08 μg·mL^{-1}, Shik 10.04 μg·mL^{-1}, Phen 10.48 μg·mL^{-1}, Hydr 3.97 μg·mL^{-1}, Chlo 16.00 μg·mL^{-1}, Feru 2.01 μg·mL^{-1}, Prot 4.97 μg·mL^{-1}, Hedt-II 21.04 μg·mL^{-1}, Betu 4.18 μg·mL^{-1}, Olea 10.72 μg·mL^{-1}, Quer 5.50 μg·mL^{-1}, Sali 4.00 μg·mL^{-1}, Dbhh 12.00 μg·mL^{-1}, Syri-II 20.12 μg·mL^{-1}, Lyon 16.00 μg·mL^{-1}, Rham-

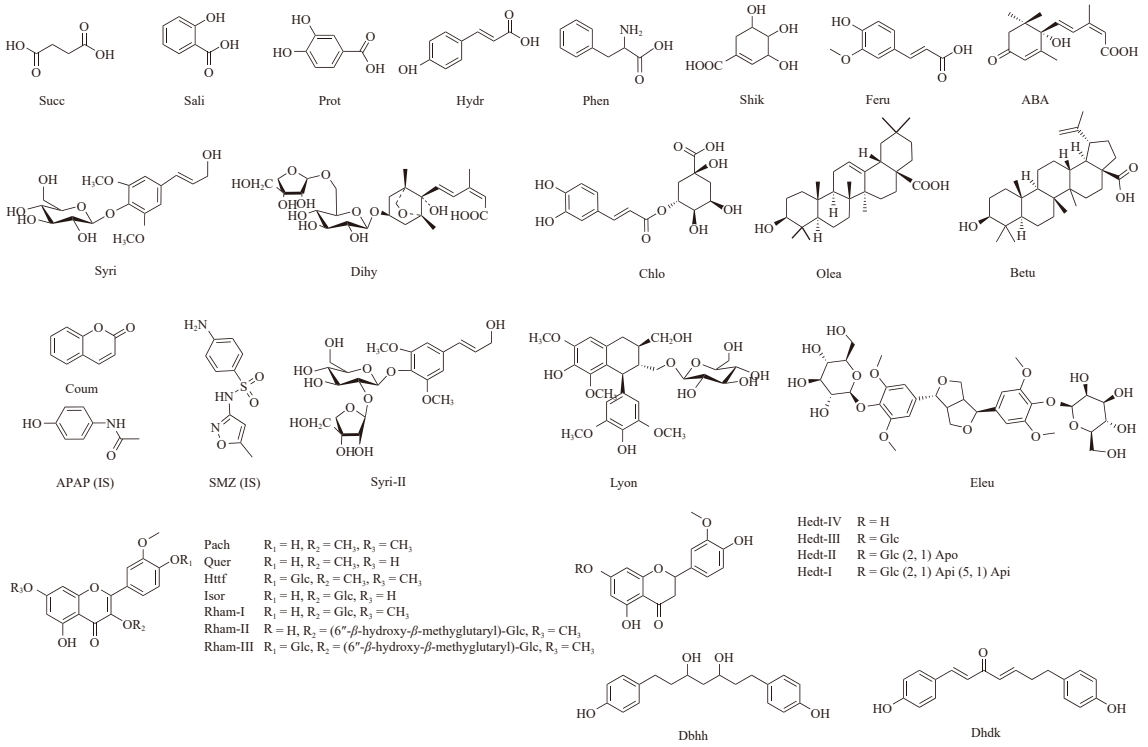

Fig. 1 Chemical structures of 30 compounds and internal standard compounds

I 1.04 μg·mL^{-1}, Rham-III 16.00 μg·mL^{-1}, Hedt-IV 18.36 μg·mL^{-1}, Hedt-III 27.05 μg·mL^{-1}, Rham-II 17.41 μg·mL^{-1}, ABA 1.02 μg·mL^{-1}, Isor 11.52 μg·mL^{-1}, Dhdk 1.12 μg·mL^{-1}, and Dihy 16.74 μg·mL^{-1}. The concentration of each compound in the positive mixed standard solution was listed as follows: Syri 2.09 μg·mL^{-1}, Pach 4.16 μg·mL^{-1}, Httf 1.05 μg·mL^{-1}, Coum 0.54 μg·mL^{-1}, and Eleu 1.05 μg·mL^{-1}.

A positive internal standard (IS) solution (20.4 ng·mL^{-1}) was obtained by dissolving accurately weighed 5 mg of SMZ in 50% methanol. Likewise, a negative IS solution was prepared by accurately weighing an appropriate amount of SMZ and APAP and dissolving in 50% methanol (SMZ 204 ng·mL^{-1} and APAP 5.2 μg·mL^{-1}).

Sample collection and preparation

V. coloratum plants were harvested every two months in Shenyang from March 2019 to January 2020, and identified by Prof. YU Zhiguo (Department of Pharmaceutical Analysis, School of Pharmacy, Shenyang Pharmaceutical University, Shenyang, China). The six host plants were marked before the first harvest to ensure the accuracy of the subsequent harvests. The samples with voucher were stored in the State Key Laboratory of Traditional Chinese Medicine (Shenyang Pharmaceutical University, China). Sample information is provided in Table 1.

Table 1 Sample number and host species of *Viscum coloratum* at different harvest times

Harvest time						Host species
2019.3	2019.5	2019.7	2019.9	2019.11	2020.1	
S3_1	S5_1	S7_1	S9_1	S11_1	S1_1	*Populus ussuriensis* Kom.
S3_2	S5_2	S7_2	S9_2	S11_2	S1_2	*Populus ussuriensis* Kom.
S3_3	S5_3	S7_3	S9_3	S11_3	S1_3	*Populus ussuriensis* Kom.
S3_4	S5_4	S7_4	S9_4	S11_4	S1_4	*Populus ussuriensis* Kom.
S3_5	S5_5	S7_5	S9_5	S11_5	S1_5	*Populus ussuriensis* Kom.
S3_6	S5_6	S7_6	S9_6	S11_6	S1_6	*Ulmus pumila* L.

The *V. coloratum* harvested in March 2019 was stored at 50 °C and 70% relative humidity for accelerated testing, and samples were obtained after 0, 1, 2, 3, and 6 months for content determination. The sampling time points were denoted as A0, A1, A2, A3, and A6.

The collected samples were dried indoors at room temperature, crushed into powder, and passed through a 4-mesh sieve. An accurately weighed 0.2 g powder was transferred to a conical flask with 20 mL 50% methanol and sonicated for 30 min. Solvent loss was compensated with 50% methanol. The extraction solution was then centrifuged at 13 000 r·min^{-1} for 10 min, and 5 mL of the supernatant was filtered using a 0.22 μm filter.

A positive ion sample solution was obtained by diluting 2.5 mL of filtered extracts and 1 mL of the positive IS solution with 50% methanol to 5 mL. Likewise, a negative ion sample solution was obtained by diluting 0.5 mL of filtered extracts and 0.5 mL of the negative IS solution with 50% methanol to 10 mL. The positive and negative ion sample solutions were stored at 4 °C prior to analysis.

Instrumental conditions

An Agilent 1290 ultra-performance liquid chromatography (UPLC) system (CA, USA) was employed for quantification. The separation was conducted on a 2.1 mm × 100 mm, 1.7 μm ACQUITY UPLC BEH C_{18} column. Mobile phase A was acetonitrile containing 0.1% formic acid, while mobile phase B was water containing 0.1% formic acid. The gradient elution program for the positive ion mode was listed as follows: 0−1 min, 5% A; 1−4.5 min, 5%−53% A; 4.5−8 min, 53%−75% A; 8−9 min, 75%−99% A; 9−11 min, 99% A. The gradient elution program for the negative ion mode was listed as follows: 0−9 min, 5%−35% A; 9−18 min, 35%−73% A; 18−23 min, 73% A; 23−23.5 min, 75%−5% A; 23.5−24 min, 5% A. The flow rate was kept at 0.25 mL·min^{-1}, and the injection volume was 5 μL. The column temperature was maintained at 35 °C, and the sample room temperature was maintained at 4 °C.

All the compounds were detected by an AB Sciex API 4000 mass spectrometer (Foster City, CA, USA). The MS parameters were set as follows: source voltage: positive ion mode, 4000 V, negative ion mode, −4000 V; source temperature (TEM), 550 °C; ion source gas1 (Gas 1), 55 psi; ion source gas2 (Gas 2), 40 psi; curtain gas, 20 psi; colliding gas, 10 psi; and dwell time, 100 ms. The MS parameters of each compound were designed and optimized for multiple reaction monitoring (MRM) mode, including precursor ion (Q1), production ion (Q3), collision energy (CE), and declustering potential (DP). The detailed conditions are shown in Supplementary Table S1. The mass spectra of the analytes are shown in Supplementary Fig. S1. All data were processed in AB Sciex Analyst 1.5.2 software.

Method performance

Specificity was tested by analyzing a 50% methanol solution, a mixed stock standard solution, and a sample solution. The positive mixed standard solution was used as positive linear standard solution SD8, while positive linear standard solutions SD7−SD1 were prepared by diluting 5, 2.5, 1.25, 0.5, 0.2, 0.1, and 0.05 mL of SD8 to 10 mL with 50% methanol. Similarly, the negative mixed standard solution was used as negative linear standard solution SD9, while neg-

ative linear standard solutions SD8−SD4 were prepared by diluting 5, 2.5, 1, 0.4, and 0.2 mL of SD8 to 10 mL with 50% methanol. Negative linear standard solutions SD3−SD1 was obtained by diluting 4, 2, and 1 mL of SD4 to 10 mL with 50% methanol. The calibration curves were established by plotting the peak area ratio of each compound to IS versus nominal concentration using the least squares linear regression analysis with a weighting factor of 1/x.

Both positive and negative linear standard solutions SD5 were analyzed six times in a day for an intra-day precision test and measured within consecutive three days for an inter-day precision test. The post-preparative stability was investigated through analyzing the same sample solution at 0, 2, 4, 6, 8, 12, and 24 h after the sample had been prepared. Furthermore, six sample solutions of S7_1 were extracted and analyzed for a repeatability test. The relative standard deviation (RSD) was evaluated in the precision, stability, and repeatability tests. In the recovery test, a standard solution was added to a sample of known content (S7_1). The amount of each compound in the standard solution was equal to that in the sample (S7_1). The accuracy of the method was evaluated using the formula: Recovery (%) = [detected amount (μg) − original amount (μg)]/spiked amount (μg) × 100%.

Results and Discussion

Method validation

The result of the specificity test is shown in Supplementary Figs. S2−S4, without apparent interferences from 50% methanol at each retention time. In this study, linear regression analysis was performed using the ratio (*Y*) of the peak area of each compound to the corresponding peak area of IS and concentrations (*X*, μg·mL^{-1}). All correlation coefficients (*R*) were greater than 0.9990. The regression equations, correlation coefficients, linear ranges, limits of detection (LODs), and limits of quantification (LOQs) are all shown in Supplementary Table S2.

All mean, SD and RSD values from the precision, repeatability and stability tests are shown in Supplementary Table S3 and S4. In the recovery test, the average recovery of the 29 compounds ranged between 91.7% and 108.3%, and all the results are shown in Supplementary Table S5. The method validation results indicated that this method was reliable, accurate, and stable for simultaneous determination of the 29 bioactive components in *V. coloratum*.

Analysis of the dynamic changes in metabolites in different harvest periods

Herein, 29 compounds in *V. coloratum* from different harvest times were determined by the established method. All the quantitative results are shown in Supplementary Table S6.

In order to illustrate the change trend of compound contents, the average content was used to draw a line graph of content changes. The Pearson correlation analysis was performed between the change trend of compound contents in each sample and the change trend of average content. Correlation coefficient (*r*) was collected in Supplementary Table S7. The correlation coefficients were almost greater than 0.7 and most of them were grater than 0.8, indicating that the average content was able to reflect the variation trend of compound content in each sample.

Metabolic pathways analysis

The possible biosynthesis pathways of the compounds were proposed according to previous literature [36, 37], and the metabolic pattern of various compounds in different growth periods were analyzed in combination with the results of quantitative analysis.

Flavonoids

The flavonoid content in different harvest periods was visualized by MeV (4.9.0), as shown in Fig. 2A. A line chart of the dynamic changes in flavonoids is shown in Fig. 3A. The possible metabolic pathways of related compounds are shown in Fig. 4A.

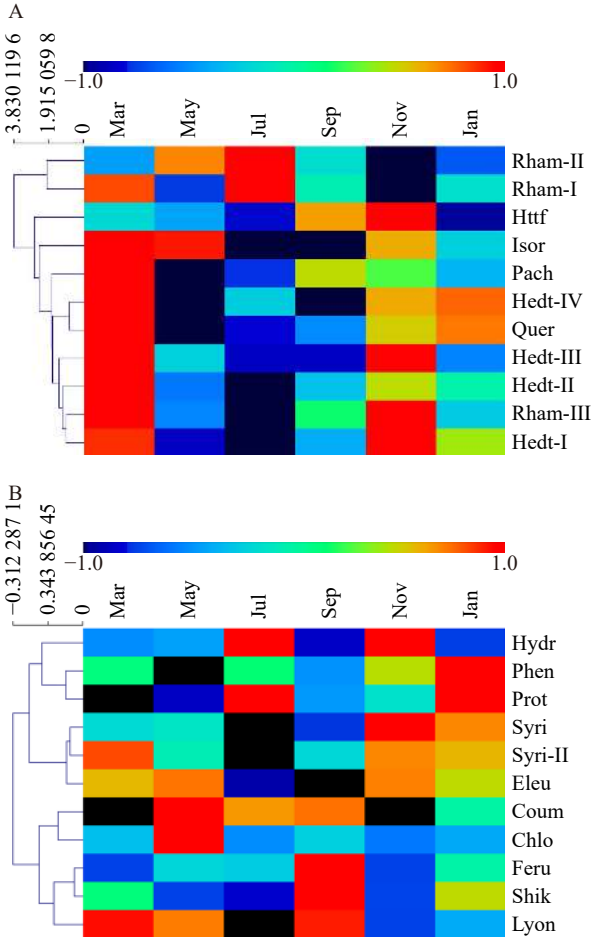

Fig. 2 Heat maps of the content of flavonoids and phenylpropanoids in different months

As indicated in Fig. 2A, except for several compounds (Rham-I, Rham-II, and Httf), the content of most compounds showed noticeable seasonal differences. Their content was generally the highest in March, but gradually decreased with the increase of the temperature. It generally reached the lowest level around July. Then, the content gradually increased with the decrease of the temperature. In autumn and winter,

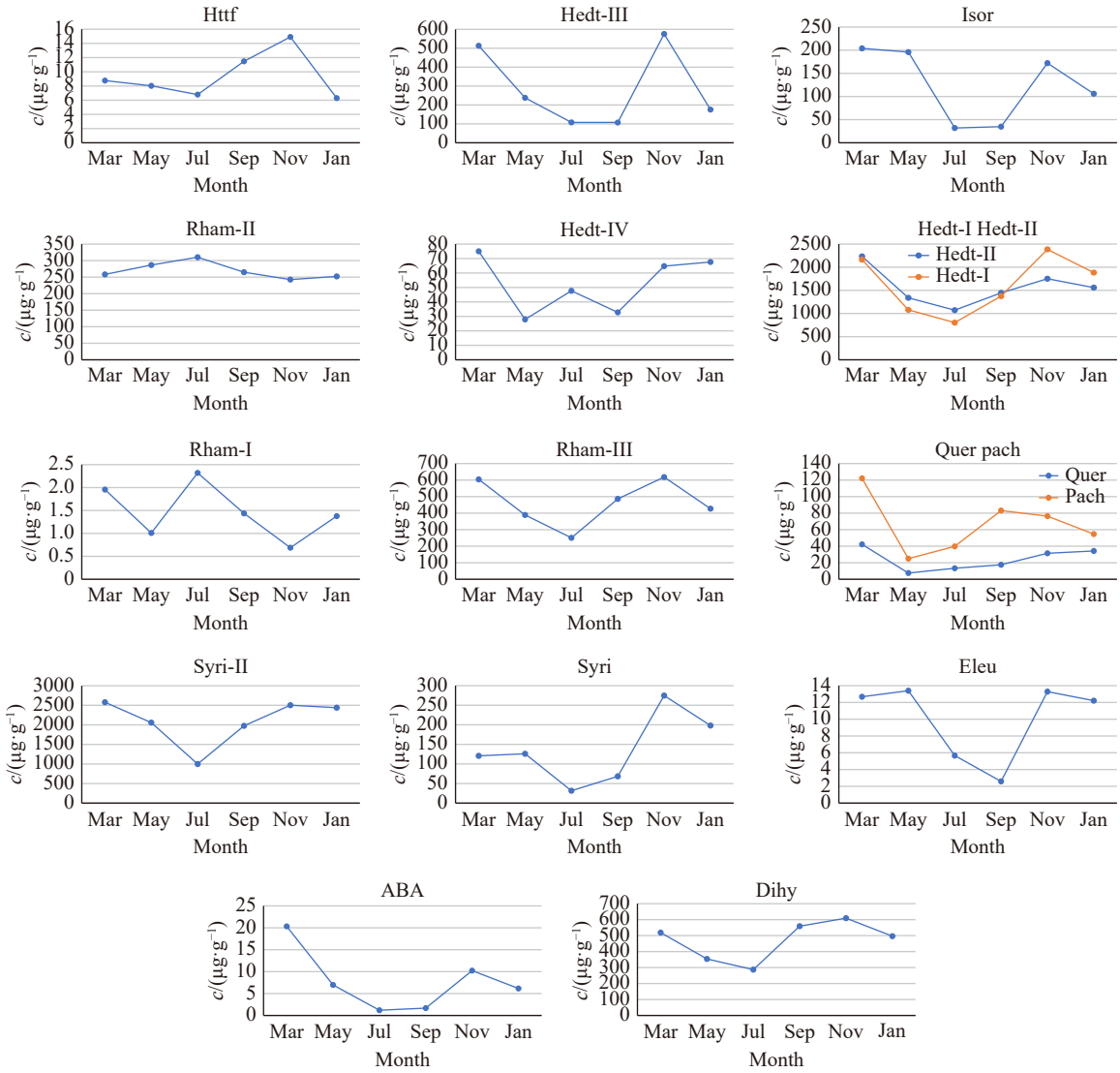

Fig. 3 Line charts of the dynamic changes of metabolites in different months

the content significantly increased. Studies have shown [38] that the synthesis of flavonoids is affected by many factors, such as light, temperature, ultraviolet radiation, and soil moisture. Sufficient light, suitable ultraviolet radiation, low temperature, and low soil moisture will increase the activity of key enzymes, such as phenylalanine aminolyase (PAL), cinnamic acid 4-hydroxylase (C4H), and 4-coumaric acid CoA Ligase (4CL) (Fig. 4A). In March, November, and January, low temperature directly stimulated related enzymes, and *V. coloratum* received sufficient light due to the shedding of the host plant leaves, resulting in more synthesized flavonoids.

The flavonoid content slightly decreased in January, especially Hedt-III, compared with those in November. January is the period when the temperature is the lowest throughout the year. Low-temperature stress is severe, and plants need to resist low temperature stress by consuming a large number of secondary metabolites. In addition, ultraviolet radiation is intense in winter. Excessively long hours of ultraviolet radiation can reduce the synthesis of flavonoids [39]. Meanwhile, the harsh environment in winter leads to insufficient nutrient supply. Therefore, a combination of these factors led to a decrease in the content of flavonoids in January.

After the basic flavonoid skeleton is formed, various flavonoids can be synthesized through a series of modifications. Essential modifications include methylation and glycosylation, which are catalyzed by oxygen methyltransferases (OMTs) and glycosyltransferases (UGTs), respectively. The possible synthetic pathways are described as follows: eriodictyol is methylated to obtain Hedt-IV, which is then glycosylated to obtain a series of dihydroflavonoid glycosides. On the other hand, eriodictyol is catalyzed by flavanone 3-hydroxylase (F3H) and flavonol synthase (FLS) to generate quercetin, which then undergoes methylation and glycosylation to form corresponding flavonoids or flavonoid glycosides (Fig. 4A).

The content of Hedt-IV was much lower than that of the

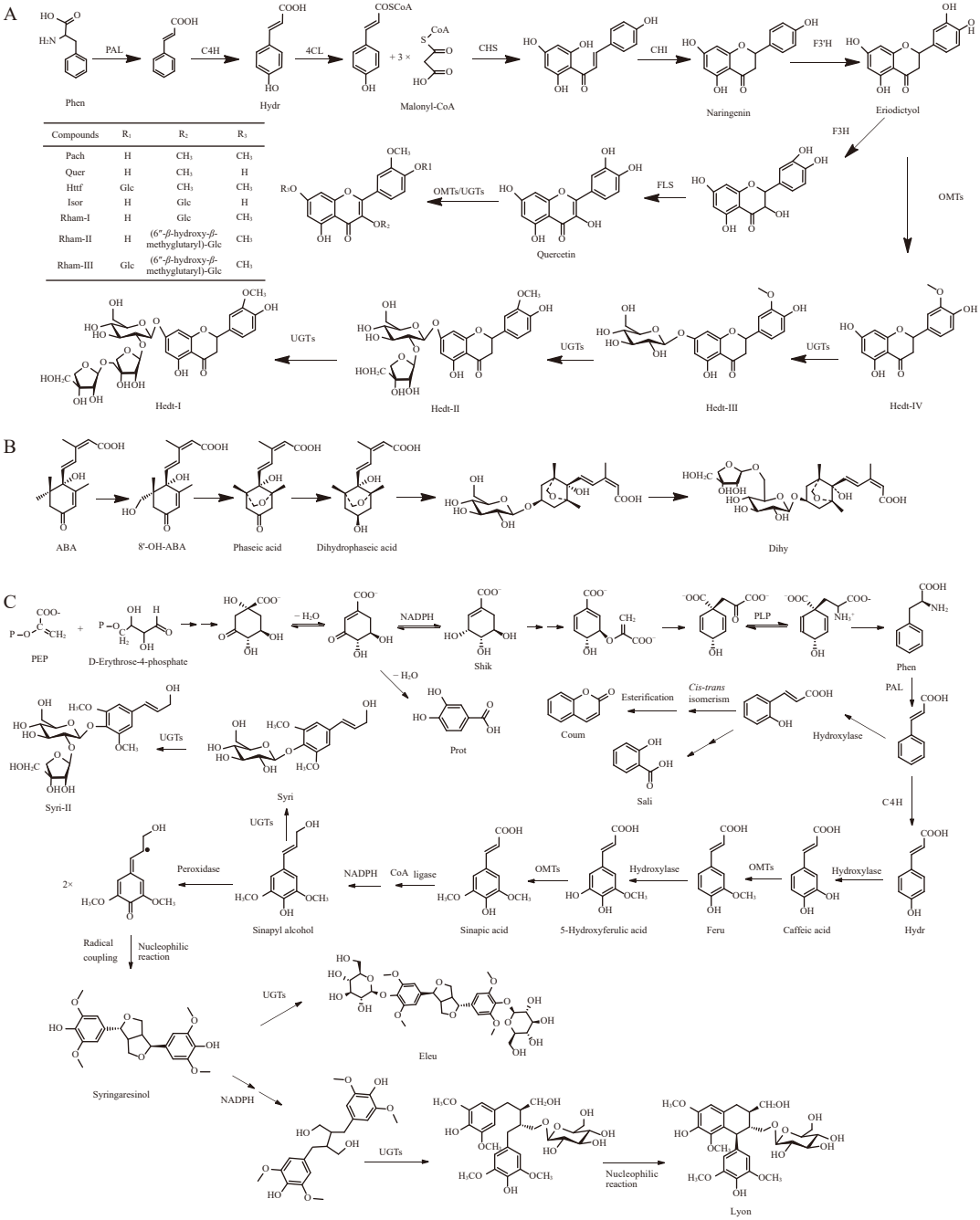

Compounds	R_1	R_2	R_3
Pach	H	CH_3	CH_3
Quer	H	CH_3	H
Httf	Glc	CH_3	CH_3
Isor	H	Glc	H
Rham-I	H	Glc	CH_3
Rham-II	H	(6″-*β*-hydroxy-*β*-methyglutaryl)-Glc	CH_3
Rham-III	Glc	(6″-*β*-hydroxy-*β*-methyglutaryl)-Glc	CH_3

Fig. 4 Possible routes of the biosynthesis of flavonoids, ABA and phenylpropanoids in *Viscum coloratum*

corresponding glycosides downstream, indicating that UGTs are more active than OMTs. After Hedt-IV is synthesized, it is glycosylated into corresponding glycosides in large amounts. Such glycosylation increases the solubility and stability of compounds and promotes the synthesis and accumulation of compounds in plants.

The content changes in Pach and Quer were similar, while the content of Quer was lower. This may be because the structure of the two compounds is similar, and they are in adjacent positions in the flavonoid metabolism network. Furthermore, as a trimethylated flavonoid, Pach is more stable, while Quer can be further methylated into Pach or glycosylated into glycosides. In addition, the content of Pach increased slightly earlier than that of other compounds in autumn and winter, and decreased earlier too. This finding suggests that the activity of OMTs related to Pach synthesis, or the expression of related genes may be more sensitive to environment conditions. Further studies concerning the related genes and enzyme activities in the biosynthetic pathway of *V. coloratum* will be carried out in the near future.

ABA and its metabolites

ABA is one of the five major plant hormones. ABA can be converted into a series of secondary metabolites through oxidation, isomerization, and esterification [36].

The main metabolic pathways are described as follows: ABA is hydroxylated to produce 8'-OH-ABA, which is then rearranged and reduced to obtain phaseicacid and dihydrosaffric acid. Dihydrosaffric acid is conjugated at the 4'-C to generate dihydrosaffric acid-4'-*O*-*β*-glucoside. Dihy may be the product of further glycosylation of dihydrosaffloric acid-4'-*O*-*β*-glucoside (Fig. 4B).

The line charts of ABA and Dihy content are shown in Fig. 3C. The ABA content was the highest in March and then gradually decreased. After September, the content began to rise. Dihy showed a similar fluctuation trend.

ABA plays a vital role in regulating plant growth and preventing against abiotic stresses, such as osmotic stress, low-temperature stress, and salt stress [40]. In winter, the temperature drops and precipitation decreases. The accumulated content of endogenous ABA will increase at a low temperature. ABA can relieve the damage of low-temperature stress to the cell membrane and reduce the content of malondialdehyde and gibberellin to improve the cold resistance of plants [41].

Decreased precipitation will cause osmotic stress to plants, which leads to dehydration and reduced water absorption. In the case of osmotic stress, the accumulation of ABA can improve plant tolerance. ABA maintains water in plants by inducing stomatal closure. Conversely, ABA can protect plants against dehydration by inducing the expression of related genes to produce biological macromolecules that protect plant cells [42].

These effects may be the main reason for the maximum accumulation of ABA in March. Additionally, ABA can also induce the ripening of seeds and fruits. September and November are the fruiting period of *V. coloratum*. This may also be a reason for the increase in ABA content in November.

Phenylpropanoids (low-molecular-weight acids, simple phenylpropanoids, and lignans)

Most phenylpropanoids are derived from phenylalanine or tyrosine. Phenylalanine (Phen) is first synthesized from phosphoenolpyruvate (PEP) and D-erythrose-4-phosphate *via* the shikimate pathway. Phen is catalyzed by phenylalanine aminolyase (PAL) to synthesize cinnamic acid, and cinnamic acid is then catalyzed by cinnamic acid-4-hydroxylase (C4H) to generate 4-hydroxycinnamic acid (Hydr). Then Hydr is modified by hydroxylation and methylation to form a series of cinnamic acid derivatives such as caffeic acid, ferulic acid (Feru), 5-hydroxyferulic acid, and sinapic acid (Fig. 4C).

Among them, p-coumaryl alcohol, pinitol, and sinapyl alcohol can be synthesized from Hydr, Feru, and sinapinic acid, respectively, through acetylation and reduction reactions. These hydroxycinnamoyl alcohol monomers can be catalyzed by peroxidase to generate free radicals, which can be coupled to form dimer lignans with various structures [37].

In this study, sinapyl alcohol produced syringin (Syri) and Syri-II through glycosylation reaction. After the formation of sinapyl alcohol free radicals, two D-type free radicals are coupled and undergo intramolecular nucleophilic attack to form syringaresinol. Eleutheroside E (Eleu) can be synthesized by the glycosylation of syringaresinin, while Lyon can be formed by the furan ring opening reaction, glycosylation, and intramolecular nucleophilic of Eleu (Fig. 4C).

The heatmaps of the content of the involved compounds are shown in Fig. 2B. As shown in Fig. 3B, the content of Syri and Eleu was low in July and September, but relatively high in other months. For syringin in particular, its content in November and January was higher than that in other months, suggesting that the synthesis of lignans and the glycosylation of sinapyl alcohol may be more active in November and January.

The content of Syri-II was significantly higher than that of Syri, indicating that more syringin was further glycosylated into Syri-II in the glucosidation reaction pathway of sinapyl alcohol.

For the other compounds, no obvious seasonality was found. It is probably because these low-molecule organic acids are located in the most upstream position in the metabolic network and can be converted into downstream products with complex structures through multiple pathways. On the other hand, the conversion between these compounds requires many steps. As the metabolic network is intricate, they will thus fail to show a clear seasonal accumulation pattern.

Comprehensive quality evaluation of V. coloratum

Since the content of various active ingredients in different months greatly varied, it was difficult to visually evaluate the quality of medicinal materials. Therefore, GRA was used for comprehensive quantitative evaluation [43].

Data standardization processing

Different component contents may not be at the same order of magnitude, and data standardization was conducted as follows. The number of measured samples was denoted as n, and the evaluation index number of each sample was denoted as m. The original data matrix $\{X_{ik}\}$ (i = 1, 2, 3$\cdots n$; k = 1, 2, 3$\cdots m$) was n = 36 and m = 29 in this paper. Original data were standardized according to Equation (1).

$$Y_{ik} = \frac{X_{ik}}{X_k} \tag{1}$$

In the equation, Y_{ik} is the standardized data and X_k is the mean value of the k-th index in 36 samples.

Selection of reference sequences

The optimal reference sequence $\{X_{wk}\}$ (k = 1, 2, 3$\cdots m$) contained the maximum value of each index measured in 36 samples. The minimum value of each index measured in 36 samples was used as the worst reference sequence, namely $\{X_{tk}\}$ (k = 1, 2, 3$\cdots m$).

Calculation of GRA

The optimal and worst reference sequence correlation coefficients were calculated according to Equations (2) and (3), respectively.

$$\zeta^i_{k(w)} = \frac{\Delta_{min} + \rho\Delta_{max}}{|Y_{ik} - Y_{wk}| + \rho\Delta_{max}} \tag{2}$$

$\Delta_{min} = \min |Y_{ik} - Y_{wk}|$, $\Delta_{max} = \max |Y_{ik} - Y_{wk}|$, Y_{wk} is the optimal reference sequence after standardization, and ρ is the resolution coefficient, generally taken as 0.5.

$$\zeta_{k(t)}^{i} = \frac{\Delta_{min} + \rho\Delta_{max}}{|Y_{ik} - Y_{tk}| + \rho\Delta_{max}} \quad (3)$$

$\Delta_{min} = \min |Y_{ik} - Y_{tk}|$, $\Delta_{max} = \max |Y_{ik} - Y_{tk}|$, Y_{tk} is the worst reference sequence after standardization, and ρ is the resolution coefficient, generally taken as 0.5.

After the correlation coefficient was obtained, the correlation degree of the optimal and worst reference sequences was calculated according to Equations (4) and (5), respectively.

$$r_{i(w)} = \frac{1}{m}\sum_{k=1}^{m}\zeta_{k(w)}^{i} \quad (4)$$

$$r_{i(t)} = \frac{1}{m}\sum_{k=1}^{m}\zeta_{k(t)}^{i} \quad (5)$$

The relative correlation degree was calculated according to Equation (6).

$$r_i = \frac{r_{i(w)}}{r_{i(w)} + r_{i(t)}} \quad (6)$$

The relative correlation degree of each sample was calculated by the above method, and the results are shown in Table 2.

According to GRA, the relative correlation degree of the samples was high in March and November, but low in July.

The results indicated that the overall quality of *V. coloratum* in March may be best, followed by November, whereas the quality of *V. coloratum* in July is the worst.

The impact of the harvest time on the biological activity of mistletoe (*Viscum album* L.) have bee investigated. For instance, Önay-Uçar [44] studied the antioxidant activity of mistletoe harvested in February and July, and found that the antioxidant activity of mistletoe was higher in February. Vicaş *et al*. [45] analyzed the antioxidant activity of aqueous extracts from mistletoe harvested in May, July, and December, and found that the antioxidant activity was the highest in December but the lowest in May. Pietrzak and Nowak [46] reported that the chemical profile and biolofical activity of mistletoe were closely related to harvest time. Mistletoe harvested in November–March had the highest total content of flavonoid and phenolic and high antioxidant activity, and autumn-winter period was the best period for mistletoe harvest. In addition, based on climate data, they found that weather conditions (such as temperature and light) might be the main underlying reason for this seasonal difference. The results of these studies are similar to the findings of this paper.

Moreover, we investigated the impact of environmental factors on the antioxidant activity of mistletoe in a previous study, and found that the antioxidant activity of mistletoe harvested in Changbai Mountain (Jilin province, China) was significantly better than that in Chengde Mountain Resort (Hebei Province, China) [32]. In the past five years, the average monthly temperature in a year in Chengde Mountain Resort was −8.3 °C to 24.68 °C, in comparison with −15.96 °C

Table 2 Relative degree of the correlation of 36 samples

Sample	r_i	r_i order	Sample	r_i	r_i order
S3-4	0.4528	1	S9-5	0.3996	19
S3-6	0.4489	2	S9-3	0.3988	20
S3-3	0.4459	3	S1-4	0.3983	21
S11-6	0.4407	4	S1-3	0.3976	22
S3-1	0.4375	5	S3-5	0.3974	23
S11-4	0.4356	6	S1-5	0.3973	24
S1-6	0.4317	7	S7-1	0.3973	25
S11-3	0.4287	8	S5-4	0.3928	26
S9-4	0.4216	9	S7-3	0.3859	27
S5-2	0.4159	10	S5-6	0.3859	28
S11-1	0.4159	11	S7-6	0.3789	29
S5-5	0.4153	12	S7-2	0.3735	30
S9-1	0.4142	13	S1-2	0.3723	31
S5-1	0.4139	14	S7-4	0.3707	32
S5-3	0.4109	15	S1-1	0.3638	33
S11-2	0.4065	16	S7-5	0.3574	34
S9-6	0.4008	17	S9-2	0.3567	35
S3-2	0.4002	18	S11-5	0.3518	36

to 21.92 °C in Changbai Mountain. Since temperature is one of the main factors of climate condition, this finding may also provide circumstantial evidence for the results of the present study. An in-depth study concerning the impact of harvest time on the biological activity (such as anti-liver fibrosis) of mistletoe will be carried out in our subsequent research.

Analysis of dynamic metabolite changes in different acceleration

Twenty-nine compounds in *V. coloratum* from different acceleration periods were determined by the established method. All the quantitative results are shown in Supplementary Table S8.

After the accelerated test, the variation trends of compound contents can be divided into three categories: reduced content (Coum, Httf, Hedt-III, Phen, Betu, Olea, Shik, Eleu, Syri, Dihy, Syri-II, Rham-III, Aba, and Hedt-I), increased content (Chlo, Dbhh, Succ, Prot, Sali, Hedt-IV, Rham-I, Rham-II, Feru, Hydr, Dhdk, and Lyon), and less change in content (Quer, Pach, Hedt-II, and Isor).

Compounds with reduced content

The line charts (Fig. 5A) indicate that the content of most compounds rapidly dropped in the first month, and then the trend flattened. However, the content of Coum and Httf first increased, but then decreased. It may be attributed to the degradation of other metabolites to produce Coum and Httf at the beginning, and then Coum and Httf were degraded.

The degradation rate of each compound at each acceleration stage is summarized in Fig. 6. The degradation rate of Eleu, Syri, Betu, Phen, Olea, and Shik exceeded 50% in the first month. After six months, the degradation rate of most components exceeded 60%, where the degradation rate of Syri and Eleu reached more than 90%.

Compounds with increased content

The components with increased content can be divided into three categories according to their change trends (Fig. 5B): Chlo, Dbhh, and Feru, which showed a rapid increase at first, followed by a decline after a plateau period; Succ, Lyon, Hydr, Dhdk, and Hedt-IV, which did not show a downward trend after increasing and plateauing; and Prot, Sali, Rham-I, and Rham-II, which showed an increasing trend during the accelerated test, without a plateau or a decline.

Compounds with less change in content

Although the content of Isor and Hedt-II slightly fluctuated, they still showed an overall degradation trend (Fig. 5C).

Most of the components with decreased contents were downstream metabolites with relative complex structures (such as Eleu, Olea, Betu, the dihydroflavonoid glycoside Hedt-I and the flavonoid glycoside Rham-III). Most of the components with increased contents were low-molecular-weight organic acids upstream of the metabolic network and simple flavonoids, such as Chlo, Succ, Prot, Feru, and the flavonoid Hedt-IV.

The results indicated that the compounds with complex structures might first degrade into some upstream compounds and some low-molecular-weight organic acids, resulting in an increase and then a decrease in the content of upstream compounds and low-molecular-weight organic acids. For example, Hedt-I and Hedt-III were deglycosylated to produce Hedt-IV, while Rham-III was deglycosylated and hydrolyzed to form Rham-I and Rham-II. In other words, the degradation of complex compounds leads to a large gap within the degradation process among different compounds.

In addition, the degradation rate of components such as eleutheroside E, syringin and oleanolic acid reached 50% within one month and exceeded 80% after six months, indicating that these components are extremely susceptible to temperature and humidity. Therefore, to ensure the quality of *V. coloratum* during storage, temperature and humidity should be strictly controlled.

The degradation rate of Eleu, Syri, Rham-III, Betu, and Shik was over 70% after the accelerated test, with a high degradation rate and a large degree of degradation. It may be attribuable to the fact that the glycosidic bonds, carboxyls, hydroxyls, and other structures in these components are easily deglycosylated, deacidified and dehydrated under high-temperature and high-humidity conditions. Therefore, these compounds were tentatively designated as "early warning components" for quality control, and special attention should be paid during drug quality control.

In summary, in this paper, the biosynthetic pathways of 29 metabolites and their dynamic changes were investigated, and the quality of mistletoe in different months was evaluated. The degradation rules of metabolites during storage were analyzed and five "early warning components" were screened.

Meanwhile, there are some questions that can be investigated in the following research. First of all, although the differences in antioxidant activity are discussed, the pharmacological effects of mistletoe are extensive, and difference analysis in more pharmacological effects (such as anti-liver fibrosis and anti-tumor activity) is need in future research, in order to provide more support for the quality assessment of mistletoe in different harvest periods. In addition, for the analysis of metabolites biosynthetic pathways and their seasonal changes, further studies concerning the related enzyme activity or DNA expression are needed to explore the molecular mechanism of seasonal changes in secondary metabolites.

Conclusions

The knowledge about the dynamic changes of secondary metabolites in plants during the growth and storage periods is crucial for rational application and storage management of medicinal materials.

In this study, the UPLC-MS/MS method was established to simultaneously determine the content of 29 components in *V. coloratum*. The associated biosynthetic pathways were reasonably speculated, and the synthesis and accumulation of different types of the compounds in different months were analyzed. A comprehensive quality evaluation of *V. coloratum* in different growth stages was performed by GRA. The

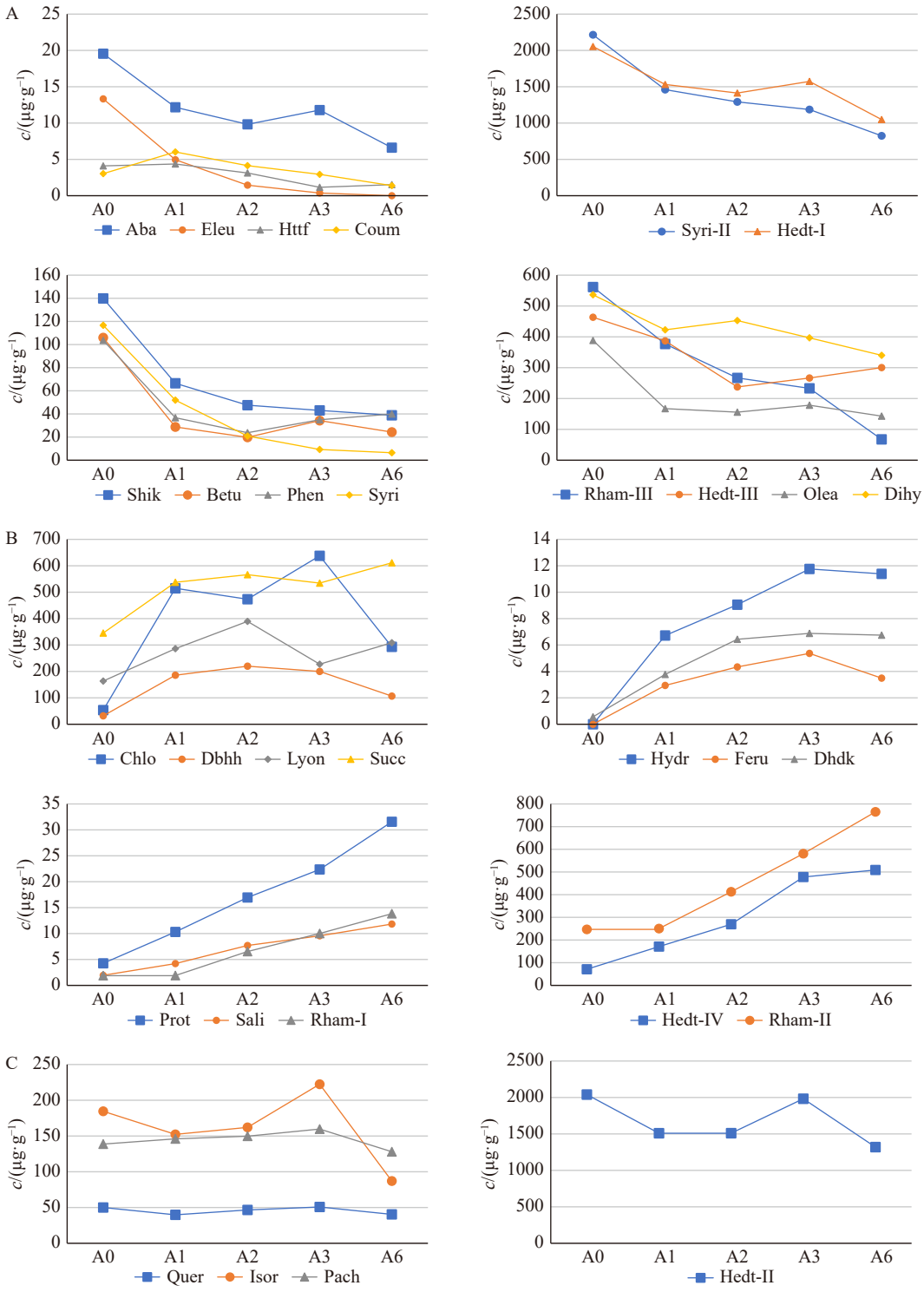

Fig. 5 Line charts of the content of each compound in the accelerated test

results indicated that the overall quality of *V. coloratum* may be the highest in March, followed by November, whereas the quality of *V. coloratum* in July is the worst.

The changes in bioactive compounds during storage were studied by the accelerated test. The results indicated that the components of *V. coloratum* are significantly affected by temperature and humidity, suggesting that special attention should be paid on temperature and humidity conditions during storage.

The change law of the metabolites can be summarized as follows: compounds with relatively complex structures in downstream steps of the biosynthesis pathway are first degraded to produce the upstream compounds and some low-molecular-weight organic acids, leading to an increase fol-

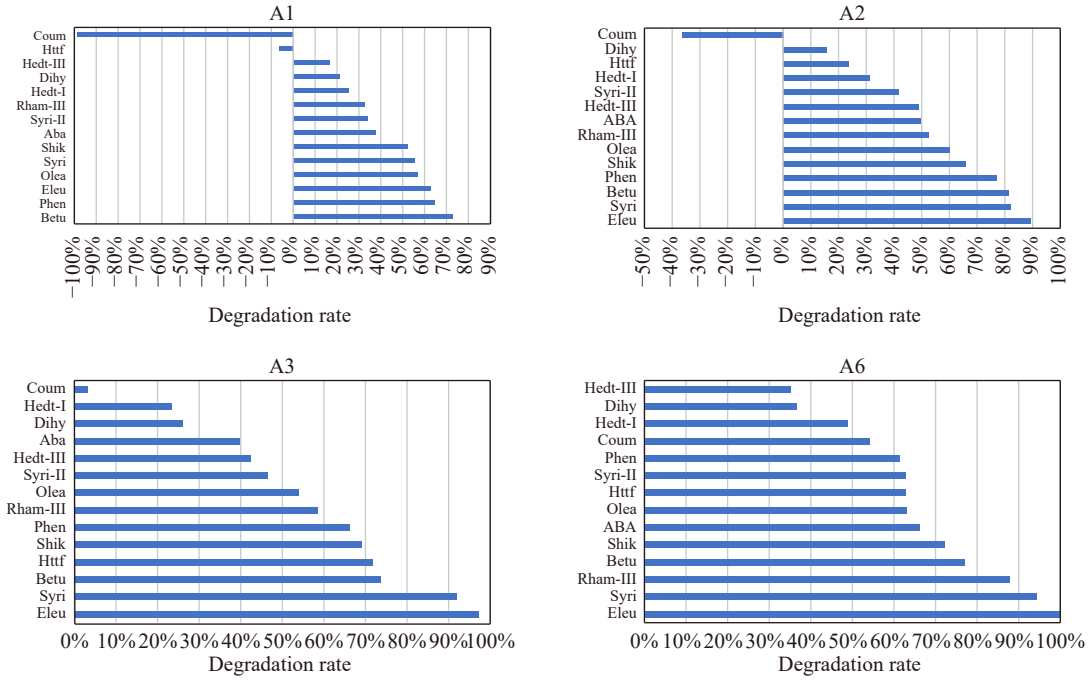

Fig. 6 Degradation rates of content-reducing components at different acceleration periods

lowed by a decrease in the content of upstream compounds and organic acids. Meanwhile, it results in a large gap during the degradation time course among different compounds. Compounds with complex structures rapidly degrade, with a relatively large degree of degradation, while those with relatively simple structures, such as small-molecular-weight organic acids, can be further degraded after a long increasing period followed by a plateau period. Active components such as syringin, betulinic acid, eleutheroside E, shikimic acid, and rhamnazin-3-*O*-*β*-D-(6"-*β*-hydroxy-*β*-methyglutaryl)-glucoside-4'-*O*-*β*-D-glucoside have a rapid degradation rate and a large degree of degradation. Therefore, these compounds are tentatively designated as "early warning components" for quality control, and requires a special focus during quality control.

This study provides reference for better understanding the biosynthesis and degradation of the metabolites in *V. coloratum* and lay a theoretical foundation for determinating the optimal harvest time and quality control of *V. coloratum* during storage. These finding will promote further studies on the rational application and quality control of Chinese herbal medicines.

Supporting Information

Supporting information of this paper can be requested by sending E-mail to the corresponding author.

References

[1] Rodríguez-Cruz ME, Pérez-Ordaz L, Serrato-Barajas BE, *et al*. Endothelium-dependent effects of the ethanolic extract of the mistletoe *Psittacanthus calyculatus* on the vasomotor responses of rat aortic rings [J]. *J Ethnopharmacol*, 2003, **86**(2–3): 213-218.

[2] Radenkovic M, Ivetic V, Popovic M, *et al*. Effects of mistletoe (*Viscum album* L., Loranthaceae) extracts on arterial blood pressure in rats treated with atropine sulfate and hexocycline [J]. *Clin Exp Hypertens*, 2009, **31**(1): 11-19.

[3] Zhang R, Shen Y, Miao S, *et al*. Protective effect of *Viscum coloratum* flavonoid glycoside on isolated myocardial ischemia-reper-fusion injury in rats [J]. *Chin Hosp Pharm J*, 2010, **30**(12): 999-1001.

[4] Fu W, Liang Z, Li T, *et al*. Effects of mistletoe lectins on tumour cells' cell cycle [J]. *J Shenyang Pharm Univ*, 2005, **22**(1): 59-70.

[5] Giudici M, Poveda JA, Molina ML, *et al*. Antifungal effects and mechanism of action of viscotoxin A3 [J]. *Febs J*, 2006, **273**(1): 72-83.

[6] Coulon A, Berkane E, Sautereau AM, *et al*. Modes of membrane interaction of a natural cysteine-rich peptide: viscotoxin A3 [J]. *Biochim Biophys Acta*, 2002, **1559**(2): 145-159.

[7] Peng H, Zhang Y, Han Y, *et al*. Studies on the anticancer effects of total alkaloid from *Viscum coloratum* [J]. *China J Chin Mater Med*, 2005, **30**(5): 381-387.

[8] Enesel MB, Acalovschi I, Grosu V, *et al*. Perioperative application of the *Viscum album* extract Isorel in digestive tract cancer patients [J]. *Anticancer Res*, 2005, **25**(6C): 4583-4590.

[9] Zai X, Wu G, Gong Z, *et al*. Studies on antioxidative substances in stem of *Viscum coloratum* [J]. *Chin Tradit Herb Drugs*, 2001, **32**(12): 1081-1083.

[10] Guan Z, Liu X, Liu H, *et al*. A novel platelet-activating factor antagonist isolated from a Chinese herbal drug *Viscum coloratum* [J]. *J Chin Pharm Sci*, 2000, **9**(2): 73-76.

[11] Yu C, Guo H. Inhibiting effects of the extacts from herbs on Human hepatitis B virus *in vitro* [J]. *Pharmacol Clin Chin Mater Med*, 2001, (1): 23-24.

[12] Huang Z, Wu X, Ren D. Isolation and identification of phenolic constituents from *Viscum coloratum* and the antiproliferative effects on A549 cells [J]. *J Shandong Univ (Health Sci)*, 2017, **55**(8): 35-41.

[13] Kong D, Luo S, Li H, *et al*. Studies on chemical components of *Viscum coloratum* I [J]. *Pharm Ind*, 1987, **18**(3): 123-127.

[14] Kong D, Luo S, Li H, *et al*. Studies on chemical components of *Viscum coloratum*: IV. Structure of viscumneoside IV [J]. *Acta Pharm Sin*, 1988, **23**(9): 707-710.

[15] Kong D, Luo S, Li H, *et al*. Studies on the chemical components of *Viscum coloratum* III. Structure of viscumneoside III,

V, and VI [J]. *Acta Pharm Sin*, 1988, **23**(8): 593-600.
[16] Kong D, Luo S, Li H, *et al*. Studies on chemical components of *Viscum coloratum* II [J]. *Pharm Ind*, 1987, **18**(10): 445-447.
[17] Kong D, Luo S, Li H, *et al*. Studies on chemical components of *Viscum coloratum* V [J]. *Chin J Pharm*, 1989, **20**(3): 108-110.
[18] Kong D, Luo S, Li H. Studies on the chemical components of *Viscum coloratum* VIII. Isolation and structure of 3-*β*-D-glucopyranosyloxy-butanol-2 [J]. *Acta Pharm Sin*, 1992, **27**(10): 792-795.
[19] Yin XM, Zhang KY, Jiang GH, *et al*. Effect of dynamic distribution of steroid saponins from *Paris polyphylla* var. *chinensis* on medical material quality [J]. *Chin Tradit Herb Drugs,* 2017, **48**(6): 1199-1204.
[20] Luo Y, Tan A, Lu S, *et al*. Determination of the content of cardiac glycoside in *Zhuang* herb *Streptocaulon griffithii* and its influencing factors of different producing areas and harvesting seasons [J]. *China Mod Med*, 2018, **25**(12): 14-17.
[21] Xue ZJ, Guo LX, Guo M, *et al*. Study on difference of chemical constituents of Qiai in different harvest periods [J]. *China J Chin Mater Med*, 2019, **44**(24): 5433-5440.
[22] Zhang Y, Xu N, Yuan Y. Impact of storage station on the quality of *Phyhalis alkekengi* L. [J]. *Chin Arch Tradit Chin Med*, 2011, **29**(6): 1282-1284.
[23] Xuan Z, Shou H, Yao H, *et al*. Effect of different drying and storing methods on quality control for leaves of *Eucommia ulmoides* [J]. *Chin Tradit Herb Drugs*, 2013, **44**(11): 1431-1434.
[24] Guo Q. *Culture of Pharmaceutical Plant* [M]. Beijing: High Education Press, 2004: 167.
[25] Ćebović T, Spasić S, Popović M. Cytotoxic effects of the *Viscum album* L. extract on Ehrlich tumour cells *in vivo* [J]. *Phyther Res*, 2008, **22**(8): 1097-1103.
[26] Dai JK, Cao D, Li CH, *et al*. Three new bioactive flavonoid glycosides from *Viscum album* [J]. *Chin J Nat Med*, 2019, **17**(7): 545-550.
[27] Fan R, Ma Y, Yuan H, *et al*. A new flavonoid glycoside and four other chemical constituents from *Viscum coloratum* and their antioxidant activity [J]. *Heterocycles*, 2014, **89**(6): 1455-1462.
[28] Zhao YL, Wang XY, Sun LX, *et al*. Cytotoxic constituents of *Viscum coloratum* [J]. *Z Naturforsch, C: J Biosci*, 2012, **67**(3–4): 129-134.
[29] Zhao YL, Fan RH, Yuan HX, *et al*. Development of the fingerprints for the quality evaluation of *Viscum coloratum* by high performance liquid chromatography [J]. *J Pharm Anal*, 2011, **1**(2): 113-118.
[30] Zhao Y, Yu Z, Fan R, *et al*. Simultaneous determination of ten flavonoids from *Viscum coloratum* grown on different host species and different sources by LC-MS [J]. *Chem Pharm Bull*, 2011, **59**(11): 1322-1328.
[31] Long C, Fan RH, Zhang QL, *et al*. Simultaneous identification and quantification of the common compounds of *Viscum coloratum* and its corresponding host plants by ultra-high performance liquid chromatography with quadrupole time-of-flight tandem mass spectrometry and triple quadrupole mass [J]. *J Chromatogr B: Anal Technol Biomed Life Sci*, 2017, **1061–1062**: 176-184.
[32] Zhang RZ, Zhao JT, Wang WQ, *et al*. Metabolomics-based comparative analysis of the effects of host and environment on *Viscum coloratum* metabolites and antioxidative activities [J]. *J Pharm Anal*, 2022, **12**(2): 243-252.
[33] Duan LX, Dai YT, Sun C, *et al*. Metabolomics research of medicinal plants [J]. *China J Chin Mater Med*, 2016, **41**(22): 4090-4095.
[34] Wang S, Hua Y, Lin Y, *et al*. Dynamic changes of metabolite accumulation in Scrophulariae Radix based on liquid chromatography–tandem mass spectrometry combined with multivariate statistical analysis [J]. *J Sep Sci*, 2017, **40**(14): 2883-2894.
[35] Zhang R, Wang W, Duan R, *et al*. Study on chemical composition of *Viscum coloratum* and its HPLC fingerprint in different harvest periods [J]. *Asian J Tradit Med*, 2020, **15**(4): 172-185.
[36] Buchanan BB, Gruissem W, Jones RL. *Biochemistry & Molecular Biology of Plants* [M]. Beijing: Science Press, 2004.
[37] Dewick PM. *Medicinal Natural Products: A Biosynthetic Approach* [M]. 2nd Ed. Wiley, 2001.
[38] Zhou M, Shen Y, Zhu L, *et al*. Research progress on biosynthesis, accumulation and regulation of flavonoids in plants [J]. *Food Res Dev*, 2016, **37**(18): 216-220.
[39] Bidel LPR, Chomicki G, Bonini F, *et al*. Dynamics of flavonol accumulation in leaf tissues under different UV-B regimes in *Centella asiatica* (Apiaceae) [J]. *Planta*, 2015, **242**(3): 545-559.
[40] Lu M, Lu G. Research progress on abscisic acid and plant abiotic stress tolerance [J]. *North Hortic*, 2014, (8): 184-188.
[41] Huang X, Chen M, Yang L, *et al*. Effects of exogenous abscisic acid on cell membrane and endogenous hormones contents in leaves of sugarcane seedling under cold stress [J]. *J Huazhong Agric Univ*, 2013, **32**(4): 6-11.
[42] Yamaguchi-Shinozaki K, Shinozaki K. Transcriptional regulatory networks in cellular responses and tolerance to dehydration and cold stresses [J]. *Annu Rev Plant Biol*, 2006, **57**(1): 781-803.
[43] Chen JL, Tan MX, Zou LS, *et al*. Stimultaneous determination of multiple bioactive constituents in Panacis Japonici Rhizoma processed by different methods and grey relational analysis [J]. *China J Chin Mater Med*, 2018, **43**(21): 4274-4282.
[44] Önay-Uçar E, Karagöz A, Arda N. Antioxidant activity of *Viscum album* ssp. *album* [J]. *Fitoterapia*, 2006, **77**(7–8): 556-560.
[45] Vicaș SI, Rugină D, Socaciu C. Comparative study about antioxidant activities of *Viscum album* from different host trees, harvested in different seasons [J]. *J Med Plants Res*, 2011, **5**(11): 2237-2244.
[46] Pietrzak W, Nowak R. Impact of harvest conditions and host tree species on chemical composition and antioxidant activity of extracts from *Viscum album* L. [J]. *Molecules*, 2021, **26**(12): 3741.

Cite this article as: ZHANG Ruizhen, DUAN Rong, WANG Weiqing, YU Zhiguo, LI Yun, ZHAO Yunli. Study on the dynamic variation of the secondary metabolites in *Viscum coloratum* using targeted metabolomics [J]. *Chin J Nat Med*, 2023, **21**(4): 308-320.